

Article

Effect of Nanodiamond Content in the Plating Solution on the Corrosion Resistance of Nickel–Nanodiamond Composite Coatings Prepared on Annealed 45 Carbon Steel

Dongai Wang ¹, Feihui Li ², Meihua Liu ^{1,*}, Wengang Zhang ³, Xiaohan Yu ¹ and Wei Da ¹¹ Department of Mechanics, Tianjin University of Commerce, Tianjin 300134, China² Department of Applied Chemistry, Tianjin University of Commerce, Tianjin 300134, China³ Tianjin Chanyu Superhard Sci-Tech Co. Ltd., Tianjin 300384, China

* Correspondence: lmhua@tjcu.edu.cn

Abstract: A nickel-nanodiamond composite coating was prepared on the surface of annealed 45 carbon steel by double-pulse electrodeposition. The effect of nanodiamond particle content on the surface morphology, grain size and wear and corrosion resistance of the composite coating were investigated. According to the analysis of the test results of X-ray diffractometry and scanning electron microscopy, it was found that the cathodic polarization of the electrodeposition process was enhanced after the addition of nanodiamond particles to the Watts nickel plating solution. The positively charged nanodiamond particles on the surface facilitate the reduction reaction at the cathode. Nanodiamond particles provide crystalline growth sites for the non-spontaneous nucleation of nickel atoms. As the addition of nanodiamond particles increases, the diffusely distributed nanodiamond particles are able to attract more nickel ions to deposit nuclei, and its fine crystallization effect increases, resulting in improved wear resistance and corrosion resistance of the composite plating. Among the results, the polarization potential was the smallest when the nanodiamond content in the plating solution was 10 g/L. The surface of the prepared nickel-nanodiamond composite coating was relatively flat and smooth, with good density and a uniform grain size distribution, and the content of element C on the surface of the composite coating was the largest, reaching 1.99%.

Keywords: carbon steel; nanodiamond; nickel composite plating; double-pulse electrodeposition



Citation: Wang, D.; Li, F.; Liu, M.; Zhang, W.; Yu, X.; Da, W. Effect of Nanodiamond Content in the Plating Solution on the Corrosion Resistance of Nickel–Nanodiamond Composite Coatings Prepared on Annealed 45 Carbon Steel. *Coatings* **2022**, *12*, 1558. <https://doi.org/10.3390/coatings12101558>

Academic Editor: Paolo Castaldo

Received: 10 September 2022

Accepted: 12 October 2022

Published: 15 October 2022

Publisher's Note: MDPI stays neutral with regard to jurisdictional claims in published maps and institutional affiliations.



Copyright: © 2022 by the authors. Licensee MDPI, Basel, Switzerland. This article is an open access article distributed under the terms and conditions of the Creative Commons Attribution (CC BY) license (<https://creativecommons.org/licenses/by/4.0/>).

1. Introduction

With the continuous emergence of new processes and technologies, as well as the rapid development of aerospace, electronic machinery, the chemical industry, automotives and other fields, some equipment parameters for mechanical components, such as wear resistance, corrosion resistance and other performance requirements, are becoming increasingly high [1]. Because of its low price, good thermal conductivity, high strength, high toughness and good wear resistance, carbon steel has been a widely used material in many fields, such as mechanical engineering, transportation, the chemical industry, pipelines, mining and construction. It is often used to manufacture high-strength moving parts, such as air compressor connecting rods, pistons, shafts, worm gears and other parts of heavy machinery. The chemical composition of carbon steel includes mainly iron. Iron is a relatively chemically active metal and is easily oxidized and corroded [2,3]. According to statistics, the annual economic loss caused by the corrosion and wear and tear of mechanical parts composed of carbon steel is approximately 3% to 5% of the total value of China's GDP [4].

To extend the life of components in the service environment and ensure their safer operation, two main measures are usually taken to improve the wear resistance, corrosion resistance and other properties of the material: improving the organization inside the carbon steel block and enhancing the surface properties of the carbon steel. Nickel plating has the advantages of high hardness, wear resistance and corrosion resistance, and is

widely used in the surfaces of parts subjected to wear and tear and sliding parts subjected to high temperatures and pressure [5–9]. Studies have shown that the performance of nickel-based composite plating, especially nickel-based nanocomposite plating, includes higher hardness, wear resistance and corrosion resistance compared to monolithic nickel plating, and it is often used as a wear- and corrosion-resistant material in industries such as precision machining, instrumentation and oil extraction [10–13]. A composite coating is composed of two phases: a base metal and dispersed particles. It combines the advantages of each component and, at the same time, avoids the disadvantages of each component. It has been shown that hard nanoparticles SiC, Al₂O₃ and nanodiamond can be electrodeposited into the nickel layer. The wear resistance of nickel composite coatings has been improved compared to monolithic nickel coatings [14–21]. In particular, nanodiamond particles are favored in composite deposition techniques due to their unique properties. Compared with nickel plating, the composite plating prepared by electrodeposition after adding nanodiamond particles to the plating solution has a uniform and dense surface, and its properties, such as hardness, wear resistance and corrosion resistance, have been greatly improved [22–26]. Therefore, it is of interest to study the nickel-nanodiamond composite plating process and to optimize the process parameters.

The research work here selects annealed treated 45 medium carbon steel as the substrate and uses the constant-current double-pulse method to investigate the effect law of nanodiamond particle content in the plating solution on the properties of nickel-nanodiamond composite coatings prepared by electrodeposition. This work provides technical support for the further optimization of the plating process to prepare high-strength and corrosion-resistant nickel-nanodiamond composite coatings by electrodeposition on the surface of medium carbon steel.

2. Preparation for Plating

2.1. Substrate Specifications

The substrate material selected was annealed 45 carbon steel with a hardness of HB195. The entire sample surface was first cleaned with degreasing cotton, and then the sample was sealed with transparent tape to form a 20 mm × 15 mm plated area with a plating area of 3 cm². The shaded area shown in the middle in Figure 1a was the test area of the plating.

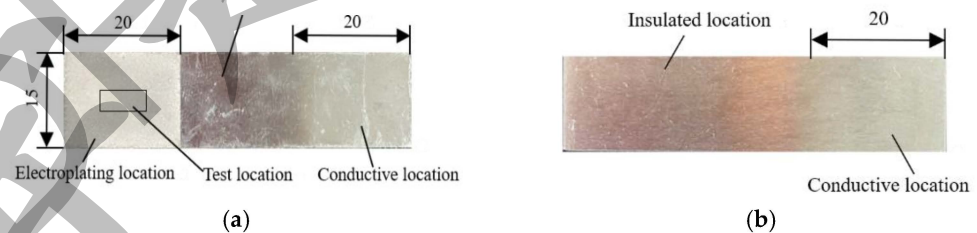


Figure 1. Schematic diagram of the substrate specification dimensions, seal location, plating area and test area: (a) front view and (b) back view.

2.2. Pre-Plating Treatment

Electrochemical degreasing of the plated part is required before plating, i.e., the plated part is used as the cathode and the platinum mesh is used as the anode. The parameters of the degreasing process were selected as follows: direct current of 10 A, temperature of 40 °C and duration of 20 s. The process of electrochemical degreasing of the plated parts was as follows: distilled water rinsing → electrochemical degreasing for 20 s → distilled water rinsing. In order to improve the bonding between the plated layer and the substrate of the plated part, the plated sample after chemical degreasing treatment was placed in a 3% dilute hydrochloric acid solution for 15 s with weak immersion, so that the surface of the plated specimen leaked the original crystal structure of the base metal. This immersion process was as follows: distilled water rinse → weak immersion for 15 s → distilled water rinse.

2.3. Testing of Cathodic Polarization Behavior and Tafel Curves

These two tests were performed using a system consisting of a three-electrode, two-loop system, in which the measurement of cathodic polarization curves was performed before the preparation of the plating. More specifically, 45 steel of the plated part was used as the study electrode, nickel plate as the auxiliary electrode and saturated glycerol electrode as the reference electrode. Watt plating solution containing nanodiamond particles was used as the electrolyte. The reference electrode was placed in a saturated potassium chloride solution so that a three-electrode, two-loop test system was formed. The two solution systems were connected by a salt bridge. One end of the Rugin capillary of the salt bridge faced the study electrode, and the other end was inserted into a saturated potassium chloride solution. The cathodic polarization curve was tested by the steady-state constant current method. The Tafel curve test was performed after the preparation of the plating. More specifically, 45 steel with a composite coating deposited on the surface was used as the study electrode, platinum-titanium mesh was used as the auxiliary electrode, and a saturated glycerol electrode was used as the reference electrode and placed in a saturated potassium chloride solution. A 3.5% NaCl solution was used as the electrolyte. The device was connected and tested with the CHI660E electrochemical workstation (Shanghai, China).

2.4. Plating Solution Components and Process Parameters

The experimental Watts plating solution was used with the following composition and content: 560 g/L of NiSO₄·6H₂O, 40 g/L of NiCl₂·6H₂O, 80 g/L of H₃BO₃, 100 g/L of CH₃(CH₂)₁₀CH₂-OSO₃Na and 4 g of activated carbon. A constant-current double-pulse electrodeposition process was used, and the plating process parameters were selected as shown in Table 1.

Table 1. Process parameters for nickel-nanodiamond composite plating by double-pulse electrodeposition.

Parameter Settings	Process Parameters	
	Positive Process Parameters	Reverse Process Parameters
On time	0.2 ms	0.1 ms
Turn-off time	0.8 ms	0.9 ms
Working time	100 ms	10 ms
Current density	0.48 A	0.03 A
Duty cycle	20%	10%
Plating solution temperature	40 °C	
Plating solution pH	3–3.5	
Plating time	70 min	
Stirring	Air pump stops and turns on every 30 s	

In order to rapidly increase the concentration of nickel ions near the cathode to reduce concentration polarization, an air pump was used for agitation during the plating process. The use of air pumps also avoids hydrogen precipitation during electrolytic deposition to reduce pinholes and pits on the plated surface.

2.5. Tests on the Performance of the Composite Coating

The nanodiamond crystal structure was tested using an X-ray diffractometer, namely, X'Pert Pro from Panalytical, Almelo, The Netherlands. Surface morphological characteristics and grain size measurements of nanodiamond particles were obtained using a scanning electron microscope, namely, LEO1530-vp produced by LEO Electron Microscopy GmbH, Jena, Germany. The surface morphology and grain size tests of the composite coating were performed with a scanning electron microscope, namely, Quanta 200 produced by FEI, Eindhoven, Netherlands, and the content of C element in the microregion of the composite coating was analyzed using the X-ray energy spectrum function of the scanning electron

microscope. The surface roughness Ra value of the composite plating was measured with a surface profiler 2302A, manufactured by Harbin Gauge & Cutting Tools Group, Harbin, China, and the density and corrosion resistance of the composite plating prepared under the conditions of differing content of nanodiamond in the plating solution were also analyzed by combining the results of the Tafel curve determination. The friction coefficients of the composite coatings were measured with the MFT-4000 multifunctional material surface property tester, products of Lanzhou HuaHui Instrument Technology Co., Lanzhou, China.

3. Analysis of Results

3.1. Effect of Nanodiamond in the Plating Solution on the Cathodic Polarization Behavior of Nickel Ions

The cathodic polarization curves of the tested nickel ions in the plating solution containing nanodiamond particles are shown in Figure 2. According to Figure 2, the polarization currents of nickel ions containing different amounts of nanodiamond particles in the plating solution are small when the cathodic potential is between -0.6 and -0.8 V. This indicates that the reduction reaction of nickel ions in the plating solution is not obvious. When the voltage is less than -0.8 V, the reduction reaction of nickel ions in the plating solution containing nanodiamond particles starts to accelerate with the decrease in voltage, and the current gradually increases. However, the reduction reaction rate of nickel ions varies with the content of nanodiamond particles in the plating solution. Among the results, the polarization potential reaches the maximum when the content of nanodiamond particles in the plating solution is 15 g/L, while the polarization potential reaches the minimum when the content of nanodiamond particles in the plating solution is 10 g/L. This indicates that when the content of nanodiamond particles in the plating solution is 10 g/L, the nickel ions in the plating solution can be better deposited on the surface of annealed 45 carbon steel and form a composite coating. According to electrochemical principles, the steeper the cathodic polarization curve, the larger the potential shift, the stronger the polarization and the more impeded the electrode process. Conversely, the smoother the polarization curve, the less polarization and the smoother the electrode process.

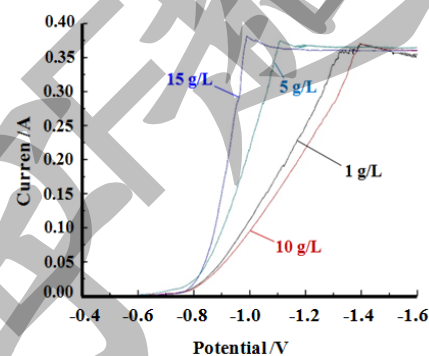


Figure 2. Curve of the effect of the presence of nanodiamond particles in the plating solution on the cathodic polarization behavior of nickel ions.

3.2. Testing of Nanodiamond Particles

The diamond particles with a scale of both micron and nanometer were dispersed into distilled water together with a dispersant. In order to ensure that the diamond particles could be fully dispersed in the distilled water, a powerful ultrasonic cleaner was applied for 2 h. Large diamond particles were then removed using a high-capacity centrifuge for 2 h at 5000 rpm. Next, a vacuum filter was used to remove the medium-grained diamonds. Finally, the dispersant carried by the remaining nanodiamond surface was removed and stably suspended in water for subsequent configuration of the plating solution.

The X-ray diffraction pattern of the nanodiamond crystal structure is shown in Figure 3. According to the determination of the face spacing of nanodiamond, the (111) face spacing of nanodiamond increased from the standard value of 0.206 to 0.207 nm, while the (220)

face spacing decreased from the standard value of 0.1261 to 0.1231 nm. The lattice of nanodiamond showed distortion. It was thus judged that the strength of the nanodiamond particles used here was higher than that of the micron-sized diamond particles.



Figure 3. Nanodiamond X-ray diffraction pattern.

The surface morphology and particle size distribution of the nanodiamond powder observed under the scanning electron microscope are shown in Figure 4. According to Figure 4, the overall observation shows that the diamond grains are unevenly distributed in size, with obvious agglomeration, and large grains are aggregated from many small grains. The proportion of grains with a size less than 100 nm in the visual inspection images is more than 90%, and the proportion of grains with a size less than 50 nm is 50%, and the grain morphology involves spherical grains. It can be seen that the agglomeration of nanodiamond powder is relatively serious. The test here revealed the state of the prepared nanodiamond powder after it was left for one month. The nanodiamond particles used in electroplating were prepared and used immediately; they were not left for a long period of time. Therefore, the dispersion of nanodiamond particles in the plating solution was better than above.

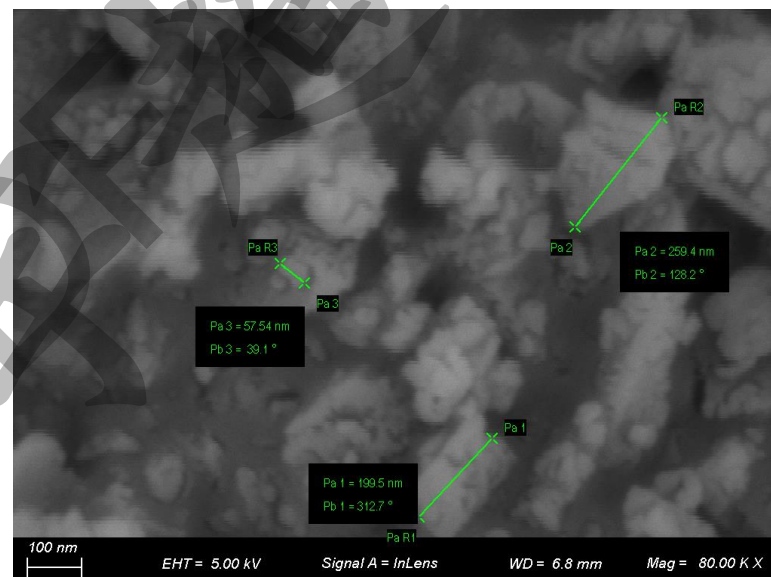


Figure 4. Scanning electron microscope image of nanodiamond powder (80,000 \times).

In order to solve the problem of agglomeration of nanodiamond particles in the plating process, three measures were taken here to solve the problem. First, surface modification of nanodiamond particles was performed during the purification of the nanodiamond, and the aqueous solution of the obtained nanodiamond particles was mixed directly with the plating solution to form a mixture. The actual dispersion of the nanodiamond particles in the plating solution thus obtained was better than in the above experimental results on the

powder. Second, the plating solution containing nanodiamond particles was ultrasonically treated to render the nanodiamond powder uniformly suspended in the plating solution before plating was performed. Third, agitation was increased during the plating process to reduce the agglomeration of nanodiamond particles in the plating solution. After taking the above three measures, the size of nanodiamond particles in the actual plating solution was smaller than that of the nanodiamond powder particles shown under the scanning electron microscope.

The agglomeration of nanoparticles in a plating solution is caused by two main forces. One type of force is caused by physical bonding (e.g., van der Waals forces) and is called soft agglomeration. The other force is agglomeration caused by chemical bonding (e.g., hydrogen bonding) and is called hard agglomeration. There are many methods to open the soft agglomerates of nanoparticles in a solution, such as mechanical stirring, magnetic stirring, gas stirring, ultrasonic dispersion, etc. To open hard agglomerates of nanoparticles in a solution, particular treatments must be applied via methods other than those described above. One of the most effective methods is the surface modification treatment of the particle surface.

3.3. Surface Morphology Analysis of the Composite Coating

Figure 5 shows the surface morphology of the composite coatings prepared at different magnifications of 1×500 , 2×2000 , 3×5000 and $4 \times 10,000$ when the content of nanodiamond particles in the plating solution was 1, 5, 10 and 15 g/L, respectively. According to Figure 5(1) ($\times 500$), when the concentration of nanodiamond in the plating solution was 1 g/L, there were a few agglomerated particles on the surface of the prepared composite layer, and the distribution was not uniform. The surface morphology of the composite layer prepared under other conditions of nanodiamond content in the plating solution was similar, i.e., the surface of the nickel composite layer showed a typical “cauliflower head” morphology. However, there was a difference in the size of the grain surface of the “cauliflower head” on the surface of the plating. Each “cauliflower head” grain was surrounded by a large number of small grains.

According to the morphological analysis of Figure 5(2) ($\times 2000$) and combined with Figure 5(3) ($\times 5000$) and Figure 5(4) ($\times 10,000$), it can be seen that the surface grains of the composite plating prepared at a nanodiamond content of 1 g/L in the plating solution have obvious angularity, and even the surfaces of the grains in the shape of the “cauliflower head” have a grain morphology similar to that of monolithic nickel. When the content of nanodiamond in the plating solution was increased to 5, 10 and 15 g/L, the surface grains of the composite plating layer were in the shape of a typical “cauliflower head”. As a whole, it was observed that the spherical grain size on the surface of the composite coating prepared at a nanodiamond concentration of 10 g/L in the plating solution was relatively uniform and the degree of projection was low.

The results of scanning electron microscopy morphology analysis of the composite plated layers showed that the surface grain morphology of the prepared composite plated layers changed with the addition of nanodiamond particles in the plating solution. This is due to the addition of sphere-like nanodiamond particles to the plating solution as a crystalline core for non-spontaneous nucleation, thus providing a large number of crystalline growth sites. The nanodiamond particles are encapsulated by the deposited nickel. In other words, the deposited nickel atoms nucleate and grow crystallographically on the surfaces of the nanodiamond particles. During the plating process, the individual grains crystallize and grow, come into contact with each other during the growth process and form clusters during the subsequent plating process. In this way, the clusters containing more grains and with a longer growth time have a larger grain size, i.e., the size of the surface of the “cauliflower head” is large; conversely, the size of the surface of the cauliflower head is small.

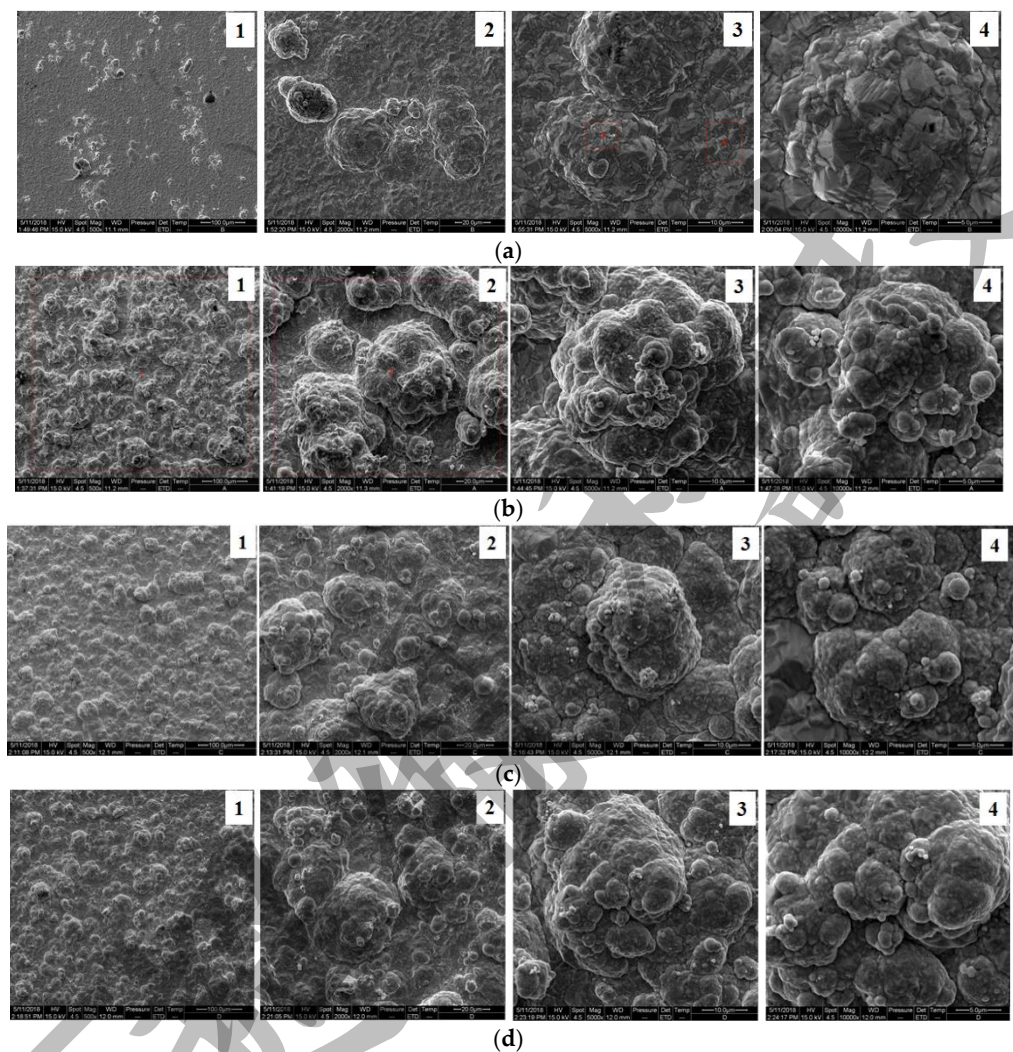


Figure 5. Scanned images of composite plating at four different magnifications (1×500 , 2×2000 , 3×5000 , $4 \times 10,000$): (a) 1 g/L, (b) 5 g/L, (c) 10 g/L and (d) 15 g/L.

3.4. Analysis of the Surface Composition of the Composite Coating

Figure 6 shows the results of the tests using the X-ray energy spectroscopy function in the scanning electron microscope. The test results showed that the main elements detected on the surface of the composite coating were C, Ni and Fe for all the composite coatings prepared under the condition of adding different amounts of nanodiamond particles in the plating solution. The content of C elements in the prepared composite coatings varied with the content of nanodiamond particles in the plating solution. The overall trend is that the content of carbon elements on the surface of the composite coating shows an increase and then a decrease with the increase in nanodiamond content in the plating solution.

In order to more accurately and objectively measure the C content on the surface of the composite plating layer, here, the elements on the surface of the composite plating layer were analyzed under the conditions of scanning electron microscope magnification of $500\times$ and $2000\times$, respectively. Finally, the average value was calculated. Figure 7 shows the relationship between the content of nanodiamond particles in the plating solution and the elemental C content of the prepared composite plating surface. According to the calculated results, the content of elemental C in the composite plating prepared under the conditions of 1, 5 and 10 g/L of nanodiamond in the plating solution showed an increasing trend of 1.3%, 1.6% and 1.99%, respectively, with the highest content of elemental C being 1.99%. The elemental C content of the composite plating prepared with a nanodiamond particle content of 15 g/L in the plating solution was 1.73%. The test results indicated a

high content of nanodiamond particles within the composite plating prepared at 10 g/L of nanodiamond in the plating solution.

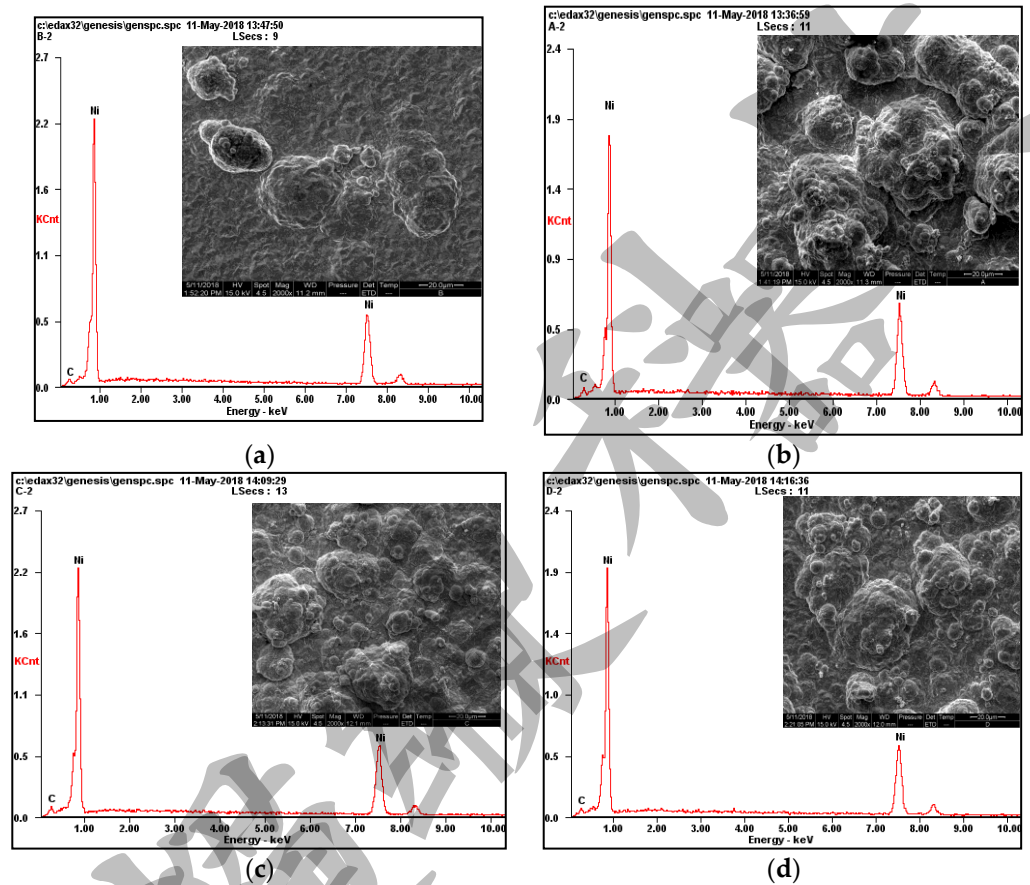


Figure 6. Scanning electron microscope energy spectrum analysis of composite plating prepared at different nanodiamond concentrations in the plating solution (2000 \times): (a) 1 g/L, (b) 5 g/L, (c) 10 g/L and (d) 15 g/L.

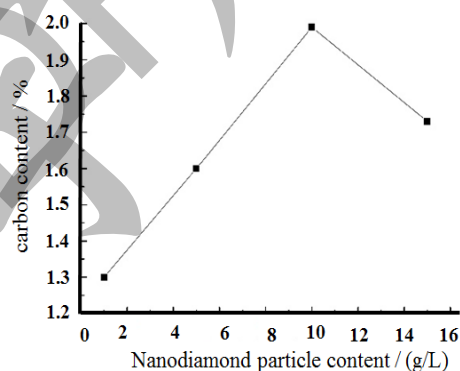


Figure 7. Nanodiamond concentration in the plating solution versus the elemental C content of the prepared composite layer.

Since some of the nanodiamond particles can be regarded as a substrate for the non-spontaneous nucleation of nickel atoms, they can attract more nickel ions to deposit nucleation and provide a large number of crystallization growth sites to achieve the effect of grain refinement. As a result, the organization of the composite layer is more refined compared to that of the normal nickel plating. Its fine crystallization effect also increases, and the grain size of the plated surface gradually decreases.

3.5. Analysis of the Corrosion Resistance and Surface Roughness of the Composite Plating

The Tafel curves of the prepared nickel-nanodiamond composite coatings were measured using a three-electrode, two-loop system, and the test results are shown in Figure 8. It can be seen from Figure 8 that the self-corrosion potentials of nickel composite coatings containing nanodiamond particles are all altered when compared with the monolithic nickel plating. The self-corrosion potential of the nickel plating is approximately -0.58 V. The polarization curve of the composite plating prepared at 15 g/L of nanodiamond particles in the plating solution shifted outside the direction of smaller potential, and the self-corrosion potential was approximately -0.64 V. In the other cases, the polarization curves of the prepared composite coatings were shifted in the direction of higher potentials, and the self-corrosion potentials were all around -0.5 V. Among them, the most positive self-corrosion potential was that of the composite plating layer prepared at 10 g/L of nanodiamond particles in the plating solution.

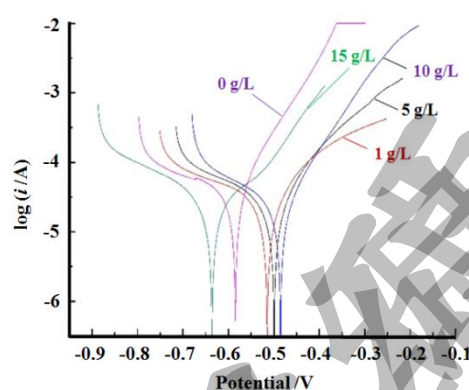


Figure 8. Tafel curves for composite coatings prepared at different diamond concentrations in the plating solution.

The addition of nanodiamond particles to the plating affects its electrochemical activity. On the one hand, the nanodiamond particles have a diffusion strengthening effect, which makes the plating denser and leads to a low void rate. Under the polarization of cathodic potential and self-corrosion potential, the surface of the sample is passivated, the electrochemical activity is reduced, and the corrosion is weakened, which inhibits the corrosion of the plating by hydrochloric acid and improves the corrosion resistance of the plating. On the other hand, when the content of nanodiamond particles in the plating solution is too high, the nanodiamond particles, which are highly prone to agglomeration, become coarser and their positive charge decreases. The actual nanodiamond content in the composite plating layer also decreases.

Figure 9 shows the relationship between the nanodiamond content in the plating solution and the surface roughness parameter R_a of the composite coating, where the black color shows the test data before the composite coating was etched and the red line shows the test results after the composite coating was etched. The general trend is that the surface of the composite coating becomes rougher after being corroded versus the surface before being corroded. The surface roughness of the composite layer tested here after corrosion is consistent with the corrosion resistance test results. More specifically, the corrosion potential of the composite layer prepared when the content of nanodiamond in the plating solution is 15 g/L is the lowest, and the difference between the surface roughness of the prepared composite layer before being corroded and that after being corroded is relatively large, i.e., the surface of the composite layer becomes rougher after being corroded. The corrosion potential of the composite layer prepared when the nanodiamond content in the plating solution was 10 g/L was the most positive. The surface roughness R_a of the composite layer before and after being corroded did not change significantly.

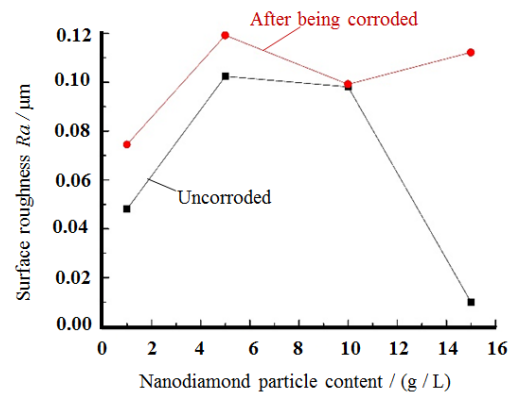


Figure 9. Surface roughness Ra of composite coatings prepared at different diamond concentrations in the plating solution before and after corrosion.

For wear- and corrosion-resistant materials, the surface roughness height parameter Ra is one of the most important measurement criteria. The surface roughness of the material is closely related to its wear resistance, corrosion resistance, fit properties, fatigue strength, contact stiffness, etc. The rougher the surface of the part, the smaller the effective contact area on the part's surface, the greater the contact pressure, the greater the friction resistance and the faster the wear. In addition, the surface roughness of the parts easily causes corrosive gases or liquids that emerge through the surfaces of the micro-grooves to penetrate into the inner layers of the parts, thus causing surface corrosion. The smaller the surface roughness value Ra of the part, the more resistant it is to wear.

3.6. Analysis of the Friction Properties of the Composite Coating

The results of the friction test on the corroded composite plating are shown in Figure 10. Figure 10a shows the trend of the friction coefficient of the composite coatings prepared with different amounts of nanodiamond particles in the plating solution with the applied load. According to Figure 10a, with the increase in external load, the friction coefficients of all four corroded composite coatings changed from large to small, and finally gradually converged to a horizontal line. When the external load was less than 10 N, the friction coefficient of the tested composite coating was relatively large, which was considered to indicate the increased friction due to the roughness of the surface of the corroded composite coating. After the external load increased to 30 N, the friction coefficients of all four composite coatings converged to a straight line, which was considered to reflect the friction coefficients of the composite coatings. Figure 10b shows the relationship between the friction coefficients of the four composite coatings tested and the nanodiamond content in the plating solution. The friction coefficients of the composite coatings prepared with nanodiamond particles in the plating solution at 1, 5, 10 and 15 g/L were 0.10, 0.11, 0.09 and 0.11, respectively. The test results listed here are essentially the same as the surface roughness measurements.

The addition of nanodiamond during electroplating changes both the grain morphology and size of the monolithic nickel. The reason is that the sphere-like nanodiamond particles act as a crystalline core for non-spontaneous nucleation to provide a large number of crystalline growth sites. The deposited nickel atoms nucleate and grow crystallographically on its surface. As the incorporation of nanodiamond particles increases, the diffusely distributed nanodiamond particles are able to attract more nickel ions to deposit nucleation, and its fine crystallization effect increases. The surface grain size of the composite coating gradually decreases, and the surface becomes flatter and denser, which improves the wear resistance of the composite coating.

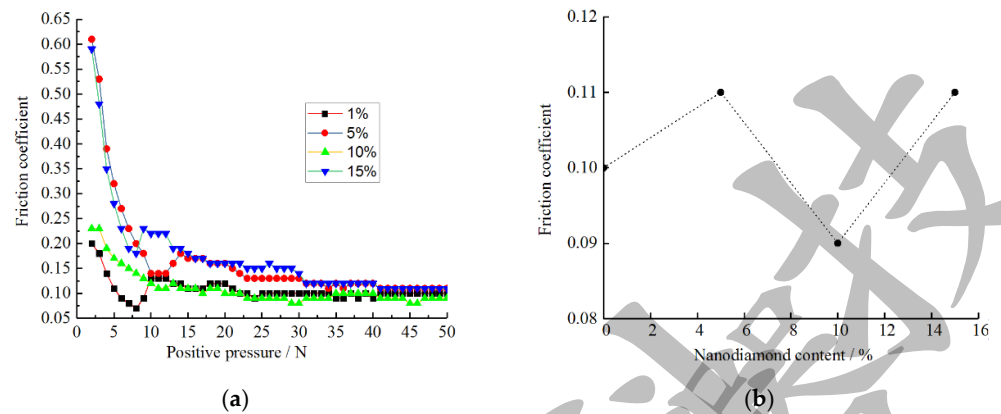


Figure 10. External load versus friction coefficient of the composite coating: (a) trend of the outermost load of the friction coefficient and (b) relationship between nanodiamond content and friction coefficient of the composite coating.

4. Conclusions

Nickel-nanodiamond composite coatings were prepared on annealed 45 medium carbon steel by constant-current double-pulse electrodeposition. The following conclusions were reached after analyzing the nanodiamond crystal structure and observing the test results of the surface morphology, grain size, friction and corrosion resistance of the prepared nickel-nanodiamond composite coatings.

- (1) The addition of nanodiamond particles to the plating solution affects the electrochemical behavior of nickel ions. The positively charged nanodiamond particles on the surface facilitate the reduction reaction at the cathode. The main reason is that the nanodiamond particles are positively charged in the wattage plating solution and the cathodic polarization is enhanced during electrodeposition. Among the results, when the content of nanodiamond in the plating solution is 10 g/L, the polarization potential is the smallest, and the nickel particles in the composite plating solution can be better electrodeposited on the substrate surface.
- (2) The surface of a nickel composite plating containing nanodiamond particles has a typical “cauliflower head” shape. As the content of nanodiamond particles increases, the grain size of the composite coating surface gradually decreases and the surface becomes flatter and denser, which improves the wear resistance of the composite coating. The main reason is that the sphere-like nanodiamond particles provide a large number of crystalline growth points as the crystalline core of non-spontaneous nucleation, which achieves the effect of effective grain refinement. The surface of the composite plating prepared with the content of 10 g/L is flat and smooth, and the grains are small and uniformly distributed. According to the scanning electron microscope energy spectrum, the highest C content of 1.99% was found on the surface of the composite coating.
- (3) The corrosion resistance of the nickel–nanodiamond composite coating was analyzed based on the results of the Tafel curves and by comparing the changes of the surface roughness parameter R_a before and after the composite coating was corroded. The results show that the nanodiamond particles alter the self-corrosion potential of the nickel composite plating. The corrosion current of monolithic nickel plating is higher than that of composite plating and is corroded faster. The general trend is that the corrosion potential shows a positive shift as the content of nanodiamond particles in the plating solution increases. The general trend is that the corrosion potential shows a positive shift as the content of nanodiamond particles in the plating solution increases. This may be related to the fineness and denseness of the grains on the surface of the composite coating due to the addition of nanodiamond.

Author Contributions: Conceptualization, M.L.; methodology, D.W. and M.L.; validation, D.W., M.L. and F.L.; formal analysis, F.L.; investigation, W.Z.; data curation, D.W. and M.L.; writing—original draft preparation, D.W. and M.L.; writing—review and editing, D.W. and M.L.; visualization, M.L.; experiment, X.Y. and W.D.; project administration, D.W. and M.L.; funding acquisition, M.L. and F.L. All authors have read and agreed to the published version of the manuscript.

Funding: This research was funded by the National Science Foundation of China, grant number 22005219.

Institutional Review Board Statement: Not applicable.

Informed Consent Statement: Not applicable.

Data Availability Statement: Not applicable.

Acknowledgments: The authors gratefully acknowledge the National Science Foundation of China (Grant No. 22005219) for providing financial support for this research work.

Conflicts of Interest: The authors declare no conflict of interest. The funders had no role in the design of the study; in the collection, analyses, or interpretation of data; in the writing of the manuscript; or in the decision to publish the results.

References

1. Zhang, Y.; Fei, J.Y.; Li, B.; Peng, Q.Y. Research progress of Ni based diamond compound coating. *Hot Work. Technol.* **2016**, *8*, 25–29.
2. Xu, Z.L.; Xia, L. *Engineering Materials*; Huazhong University of Science and Technology Press: Wuhan, China, 2020; Volume 8.
3. Wu, G.H.; Shen, J.X.; Zhuang, L. *Metal Materials & Heat Treatment*; Beijing University of Technology Press: Beijing, China, 2018; Volume 8.
4. Zhang, M.X. Preparation and Tribological Properties of Electroless Ni-B Coating on 45# Steel Substrates. Master's Thesis, Qingdao University of Technology, Qingdao, China, 2015.
5. Lin, C.S.; Hsu, P.C.; Chang, L.; Chen, C.H. Properties and microstructure of nickel electrodeposited from a sulfamate bath containing ammonium ions. *J. Appl. Electrochem.* **2001**, *31*, 925–933. [[CrossRef](#)]
6. Prasanta, S.; Suman, K.D. Tribology of electroless nickel coatings—A review. *Mater. Des.* **2011**, *32*, 1760–1775. [[CrossRef](#)]
7. Bai, X.C.; Liang, G.X.; Lv, M. Micromorphology and wear resistance of selective electrochemically deposited nickel coating. *Heat Treat. Met.* **2021**, *46*, 142–148.
8. Yuan, X.T.; Wang, Y.; Sun, D.B.; Yu, H.Y. Influence of pulse parameters on the microstructure and microhardness of nickel electrodeposits. *Surf. Coat. Technol.* **2008**, *202*, 1895–1903. [[CrossRef](#)]
9. Walsh, F.C.; Ponce de Leon, C. A review of the electrodeposition of metal matrix composite coatings by inclusion of particles in a metal layer: An established and diversifying technology. *Trans. IMF* **2014**, *92*, 83–98. [[CrossRef](#)]
10. Peeters, P.; Hoorn, G.V.D.; Daenen, T.; Kurowski, A.; Staikov, G. Properties of electroless and electroplated Ni-P and its application in microgalvanics. *Electrochim. Acta* **2001**, *47*, 161–169. [[CrossRef](#)]
11. Guo, C.; Zuo, Y.; Zhao, X.; Zhao, J.; Xiong, J. Effects of surfactants on electrodeposition of nickel-carbon nanotubes composite coatings. *Surf. Coat. Technol.* **2008**, *202*, 3385–3390. [[CrossRef](#)]
12. Chou, M.C.; Ger, M.D.; Ke, S.T.; Huang, Y.R.; Wu, S.T. The Ni-P-SiC composite produced by electro-codeposition. *Mater. Chem. Phys.* **2005**, *92*, 146–151. [[CrossRef](#)]
13. Cai, C.; Zhu, X.B.; Zheng, G.Q.; Yuan, Y.N.; Huang, X.Q.; Cao, F.H.; Yang, J.F.; Zhang, Z. Electrodeposition and characterization of nano-structured Ni-SiC composite films. *Surf. Coat. Technol.* **2011**, *205*, 3448–3454. [[CrossRef](#)]
14. Gang, W.; Ning, L.; Derui, Z.; Kurachi, M. Electrodeposited Co-Ni-Al₂O₃ composite coatings. *Surf. Coat. Technol.* **2004**, *176*, 157–164. [[CrossRef](#)]
15. Zhang, X.; Qin, J.; Perasinjaroen, T.; Aeksen, W.; Das, M.K.; Hao, R.; Zhang, B.; Wangyao, P.; Boonyongmaneerat, Y.; Limpanart, S.; et al. Preparation and hardness of pulse electrodeposited Ni-W- diamond composite coatings. *Surf. Coat. Technol.* **2015**, *276*, 228–232. [[CrossRef](#)]
16. Vaezi, M.R.; Sadrnezhaad, S.K.; Nikzad, L. Electrodeposition of Ni-SiC nano-composite coatings and evaluation of wear and corrosion resistance and electroplating characteristics. *Colloids Surf. A Physicochem. Eng. Asp.* **2008**, *315*, 176–182. [[CrossRef](#)]
17. Soleimani, R.; Mahboubi, F.; Kazemi, M.; Arman, S.Y. Corrosion and tribological behaviour of electroless Ni-P/nano-SiC composite coating on aluminium 6061. *Surf. Eng.* **2015**, *31*, 714–721. [[CrossRef](#)]
18. Luo, H.; Leitch, M.; Behnamian, Y.; Ma, Y.; Zeng, H.; Luo, J.L. Development of electroless Ni-P/nano-WC composite coatings and investigation on its properties. *Surf. Coat. Technol.* **2015**, *277*, 99–106. [[CrossRef](#)]
19. Walsh, F.C.; Low, C.T.J.; Bello, O. Influence of surfactants on electrodeposition of a Ni- nanoparticulate SiC composite coating. *Trans. IMF* **2015**, *93*, 147–156. [[CrossRef](#)]
20. Tamilarasan, T.R.; Rajendran, R.; Rajagopa, G.; Sudagar, J. Effect of surfactants on the coating properties and corrosion behavior of Ni-P-nano-TiO₂ coatings. *Surf. Coat. Technol.* **2015**, *276*, 320–326. [[CrossRef](#)]

21. Grosjean, A.; Rezrazi, M.; Takadom, J.; Bercot, P. Hardness, friction and wear characteristics of nickel-SiC electroless composite deposits. *Surf. Coat. Technol.* **2001**, *137*, 92–96. [[CrossRef](#)]
22. Hamed, M.; Saeed, A. Deposition characterization and electrochemical evaluation of Ni-P-nano diamond composite coatings. *Appl. Surf. Sci.* **2012**, *258*, 4574–4580. [[CrossRef](#)]
23. Luan, X.W.; Wang, M.Z.; Zhao, Y.C. Study on electroplated nickel-nanodiamond composite coating. *Diam. Abras. Eng.* **2005**, *150*, 20–22.
24. Wang, J.; Zhang, F.L.; Zhang, T.; Liu, W.G.; Li, W.X.; Zhou, Y.M. Preparation of Ni-P-diamond coatings with dry friction characteristics and abrasive wear resistance. *Int. J. Refract. Met. Hard Mater.* **2018**, *70*, 32–38. [[CrossRef](#)]
25. Petrov, I.; Detkov, P.; Drovosekov, A.; Ivanov, M.V.; Tyler, T.; Shenderova, O.; Voznecova, N.P.; Toporov, Y.P.; Schulz, D. Nickel galvanic coatings co-deposited with fractions of detonation nanodiamond. *Diam. Relat. Mater.* **2006**, *15*, 2035–2038. [[CrossRef](#)]
26. Bi, X.Q.; Wei, Y.L. Effects of addition of nano-diamond on structure and properties of Ni-P composite coating of magnesium alloy. *Surf. Technol.* **2016**, *12*, 68–72.